14[th] International Conference on Applications of Statistics and Probability in Civil Engineering, ICASP14
Dublin, Ireland, July 9-13, 2023

A Discrete Element-Based Monte Carlo Study for the Calibration of Cyclic Soil Degradation Models for Saturated Sands

Alessandro Tombari
Senior Lecturer, Architecture, Technology and Engineering, University of Brighton, Brighton, UK

Pierfrancesco Cacciola
Reader, Architecture, Technology and Engineering, University of Brighton, Brighton, UK

Fedor Maksimov
PhD Student, Architecture, Technology and Engineering, University of Brighton, Brighton, UK

ABSTRACT: Saturated sands under fast cyclic loading can experience excess pore pressure build-up that progressively deteriorates the geotechnical characteristics of the soil sample, such as strength and stiffness. In extreme cases, the soil can manifest the liquefaction phenomenon. Past laboratory cyclic loading triaxial tests have shown that the main factors affecting this phenomenon are the particle size distribution, the initial void ratio, the confining pressure and the magnitude of cycle stress or strain. Moreover, in real soil, these factors can be considered uncertain due to the inherent soil variability as well as the random nature of the dynamic load. Therefore, to investigate thoroughly the impact of these factors on the soil degradation, a large number of experimental tests would be required. On the other hand, the Discrete Element Method (DEM) offers an interesting and fast numerical approach to simulate cyclic undrained triaxial testing. Therefore, thanks to the potentiality of this method, a multitude of numerical analyses can be conducted in a shorter time frame. This paper presents a statistical-based cyclic degradation model which can be used to predict the degradation of the maximum shear stress of saturated sands. Statistical moments will be determined through a pertinent Monte Carlo Simulation of DEM cyclic triaxial testing. Analytical expression of probability density functions will be derived using the Maximum Entropy principle using the first four statistical moments. Finally, statistical regression analysis is used to calibrate the parameters of an elliptical soil damage model considering the randomness of the grain distribution.

1. INTRODUCTION

Offshore wind turbine (OWT) foundations are continuously subjected to cyclic loading induced by wind and waves and occasionally, earthquakes. Therefore, soil fatigue assessment is fundamental and typically represents the driver factor in the design of an OWT foundation. Although several non-generally accepted standardised approaches exist for the evaluation of the cyclic load-bearing capacity (Shajarati et al. 2012), the current standards prescribe mandatory dynamic time-history analyses to capture the effect of the cyclic loading on the hardening or softening of the soil-foundation system (Schafhirt et al., 2016). Therefore, advanced numerical constitutive models are required to be able to assess soil fatigue.

Basically, cyclic soil degradation and hardening can be linked essentially to the increase or decrease in the mean effective confining stress; in drained conditions this phenomenon is linked to the variation of the void ratio, whilst under undrained conditions, typical for an OWT foundation, it is caused by the excess pore pressure build-up. The changes in the internal state of the soil can be explicitly modelled by using effective stress methods, i.e., with a fully coupled soil skeleton – pore fluid scheme or implicitly modelled using total stress methods. This last approach normally requires the use of empirical functions describing the relation between constant-amplitude stress or strain cyclic loads and the number of cycles, and hence, they can be defined as soil fatigue-based problems.

Under this class of problems, several formulations have been proposed in the past, such as the Linear Damage Accumulation (Van Eekelen 1977) and the Palmgren–Miner cumulative damage and various models have been applied directly to simulate the degradation of the soil-pile system; for instance, Allotey and El Naggar (2007), proposed a consistent soil fatigue framework that has been implemented in a generalized dynamic Winkler model (Allotey and El Naggar, 2008).

These approaches can be calibrated through cyclic laboratory soil testing such as cyclic triaxial or cyclic simple shear tests. On the other hand, several factors affect the cyclic soil behavior such as the particle size distribution, the initial void ratio, the confining pressure and the magnitude of cycle stress or strain; therefore, in order to investigate thoroughly the impact of each factor on soil degradation, a large number of experimental tests would be required.

Maksimov and Tombari, (2022) showed that the Discrete Element Method (Cundall and Strack 1979) can provide interesting and fast numerical support in investigating the impact of these parameters through numerical cyclic undrained triaxial testing. In this paper, calibration of the Allotey and El Naggar's fatigue model (2007), is conducted by performing Monte Carlo Simulation of cyclic triaxial testing through the Discrete Element Method (DEM). The inherent randomness of the particle size distribution of a saturated sand is considered.

The DEM model is first calibrated through experimental tests carried out by ElGhoraiby et al. (2020) for the Liquefaction Experiments and Analysis Project (LEAP); this was a collaborative research project to provide experimental data for calibration and verification of constitutive models for finite element modelling. Therefore, numerical cyclic triaxial testing is conducted on several realizations of particle size distribution functions with increasing degrees of uncertainty. The results in terms of fatigue and degradation curves are used to obtain the probability distribution functions of the parameters involved in the Allotey and El Naggar, (2007) soil fatigue model.

2. OTTAWA F65 SAND SOIL CHARACTERIZATION

The soil investigated in this paper is the Ottawa F-65 sand which has been comprehensively investigated in the LEAP (Kutter et al. 2020). It is an inert, white silica sand of rounded grains with a quartz content of 99.7%. The Ottawa F-65 sand is classified as poorly graded sand with a fine content less than 0.5%; the average particle size distribution is given in Figure 1.

The characterization of the sand has been carried out on samples that were dry pluviated during sample preparation and saturated before the consolidation stage of testing. The average specific gravity of the samples was determined to be 2.65; the median values of maximum and minimum void ratios, i.e., e_{max} = 0.78 and e_{min} = 0.51, will be considered in the present paper.

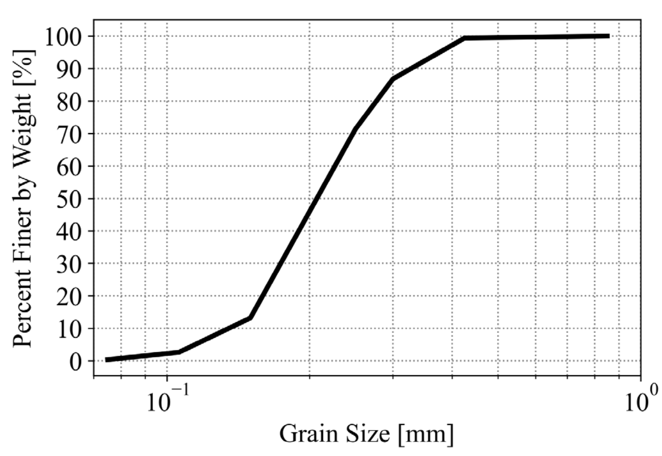

Figure 1. Ottawa F65 – Particle Size Distribution

3. NUMERICAL CYCLIC TRIAXIAL TESTING

3.1. Contact Law

The Discrete or Distinct Element Method (Cundall and Strack 1979) is based on the analysis of the dynamic equilibrium of an assembly of particles stressed by the movement of the model boundaries. The force-displacement relation between 2 touching particles of radii r_i and r_j is described through the Cundall-Strack elastic perfectly brittle contact law. For each interaction between 2 particles, the forces exchanged at the contact point are the normal force, $F_n = k_n \cdot d_n$, the tangent force, $F_t = -k_s \cdot d_t = -\nu \cdot k_n \cdot d_t$ and the increment of rolling torque $\Delta M = -\alpha \cdot k_s \cdot r_i \cdot r_j \cdot \Delta\theta_{ij}$, where d_n is the normal overlapping distance of the contacting spheres, d_t is the tangential displacement and $\Delta\theta_{ij}$ the incremental relative rolling rotation of two particles. The remaining parameters are described in Table 1; the Mohr–Coulomb rupture criterion is considered for the modelling of the cohesionless soil, hence, $\|F_t\| \leq \|F_n\| \tan \mu$ and $\|M\| \leq \|F_n\| \eta_r \min(r_i, r_j)$. In this paper, the Poisson's ratio of the contact law is fixed at 0.2 while the other 4 parameters in Table 1 are calibrated from the experimental cyclic triaxial testing experimental performed for the LEAP (see Section 4).

3.2. Numerical Consolidation Phase

The open-source code YADE (Kozicki and Donzé 2008) is used for the modelling and simulation of the cyclic triaxial testing. The particles have been randomly generated according to the given particle size distribution function in Figure 1 which has been used as cumulative distribution function. Then, the assembly is created by enclosing the random cloud of particles enclosed in a cubic cell of 0.04m size.

The resulting packing is a gas-like state with no contacts. A period boundary condition is used for modelling the cell boundaries. The cloud of particles is then subjected to isotropic compression by moving uniformly the cell boundaries until the mean stress reaches the desired confining pressure. At this point, the interparticle friction angle is reduced to decrease the void ratio by keeping a constant confining pressure. The procedure stops when both confining pressure and void ratio reach the target values. After this procedure, the initial parameter of interparticle friction angle is assigned. The reference sample used in this paper is characterized by an initial void ratio of 0.608 and confining pressure of 100kPa.

3.3. Strain-Controlled Cyclic Triaxial Testing

The second phase is the strain-controlled cyclic triaxial testing. The assembly of particles is then subjected to cyclic deviatoric stress induced by controlling the strain levels of the sample boundaries. It is worth mentioning that the pore pressure is not modelled, hence, to simulate the undrained conditions, a constant volume (undrained condition) is obtained by constraining the strains in the three directions as follows (Martin et al. 2020, Maksimov and Tombari 2022):

$$\varepsilon_{xx} = \varepsilon_{yy} = -0.5 \cdot \varepsilon_{zz} \tag{1}$$

in which ε_{xx} and ε_{yy} are the strains of the lateral boundaries of the periodic cell, whilst ε_{zz} is the axial strain aligned the cyclic direction during the triaxial testing.

The cyclic behavior is then imposed through the following relation:

$$\dot{\varepsilon} = \varepsilon_{zz}^{max} \cdot 2\pi f \cdot \cos(2\pi f t) \tag{2}$$

where f is the frequency (fixed at 0.0083 Hz as in Kutter et al. 2020), ε_{zz}^{max} is the maximum deviatoric strain, t is the current time in seconds.

Table 1. Cundall-Strack Law: Model Parameters

Parameter	*Description*	*Value*
k_n	*normal stiffness N/m*	$6.0E8$
ν	*Poisson's ratio*	0.2
α	*rolling stiffness coefficient*	2
μ	*Frictional angle*	17°
η_r	*limiting rolling coefficient*	0.15

Figure 2a shows for a randomly-selected sample, the cyclic deviatoric stress- axial strain behavior showing the typical cyclic softening of saturated sands. The simulation continues indefinitely till the maximum deviatoric stress at each cycle is reduced to the 10% of the maximum deviatoric stress recorded at the first cycle. Figure 2b shows the reduction of mean and the deviatoric stresses with the number of cycles till liquefaction is initiated (mean stress ≅ 0).

4. CALIBRATION OF THE DEM PARAMETERS

4.1. Morris Sensitivity

To understand the importance of each factor on the testing outcome, i.e., the number of cycles to liquefaction, the Morris sensitivity, or Elementary Effects Method, is applied. This method belongs to the global "Once-At-Time" class and is an effective way of screening the important parameters of a model. The method consists of the generation of r trajectories where in each one, the $k$parameters are changed randomly only once by a pre-defined value function of the number of levels, p, for the discretization. Each point of the trajectories represents each evaluation of the model. Results are analyzed statistically in terms of the mean of the absolute value of the elementary effects to avoid Type II errors. The mean value allows to assess the overall influence of each factor on the output, ranking from the most to the least important; the standard deviation estimates the ensemble of the factor's effects due to nonlinearities and interactions with other factors. The method is exhaustively explained in Saltelli et al., (2007).

In this paper, $r = 50$ trajectories have been generated for the $k = 4$ parameters with $p = 6$ levels of discretization. The ranges of variation of the parameters that have been tested are $k_n = [4E8 - 2E9]$, $\mu = [10^{\circ} - 35^{\circ}]$, $\eta^r = [0 - 0.4]$ and $\alpha = [0 - 3]$ in according to past DEM analyses (Maksimov and Tombari 2022). The ranking of the factors is shown in Figure 3, showing that although the importance of the rolling stiffness coefficient is prevalent, all the 4 parameters should be taken into consideration for the calibration of the model.

4.2. Heuristic Approach

As observed in Figure 3, all the 4 parameters should be considered for the calibration of the contact law. The experimental $e_z - N_u$ curve (strain-number of cycles to liquefaction) is used as reference curve for the calibration of the DEM model. In the first instance, a heuristic approach is used; the method consists of two steps, first calibration of the parameters, k_n and μ, to obtain the maximum deviatoric stress and initial stiffness of the backbone curve through a monotonic analysis (if experimental data are available) and then, cyclic triaxial testing to obtain the target number of cycles to liquefaction by changing the parameters α and η_r.

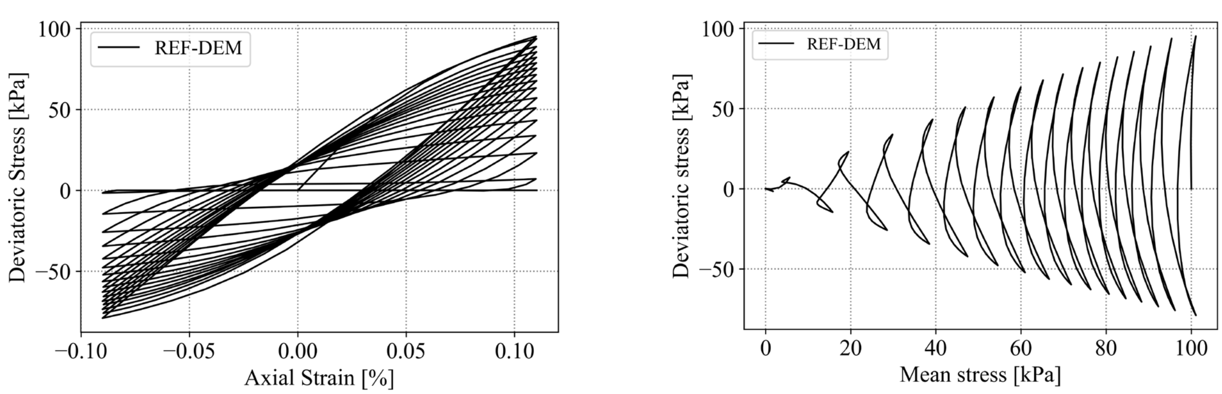

Figure 2. Numerical Cyclic Triaxial Test for a randomly-selected sample: a) stress-strain hysteresis and b) variation of the deviatoric and mean stress with the increase of the number of cycles

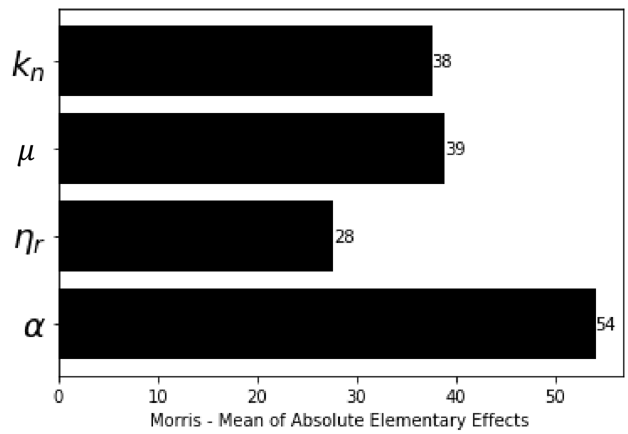

Figure 3. Ranking of the DEM parameters obtained through Morris sensitivity analysis

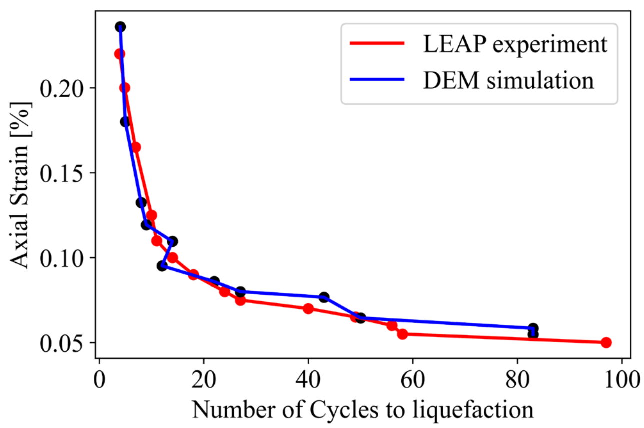

Figure 4. Calibration of the DEM model against the experimental $e_z - N_u$ curve (Kutter et al. 2020)

These two values related to the particle rolling are changed till the convergence of the result for one axial-strain level. The two steps are then repeated iteratively in order to obtain a good approximation of the reference curve, such as in Figure 4. It is worth noting that the number of cycles for each strain level is an independent DEM analysis. Calibrated values are reported in Table 1.

5. RANDOM CYCLIC DAMAGE MODEL

The degradation model considered in this paper is the stress-independent elliptical function proposed by Allotey and El Naggar (2008) which is described by the following formula:

$$\delta_s = 1 + (\delta_f - 1)\left[1 - (1-D)^{\theta}\right]^{\frac{1}{\theta}} \qquad (3)$$

where δ_s is the strength degradation index, $\delta_f = 0.1$ is the liquefaction onset limit, θ is an empirical curve shape parameter and D is the damage factor. The strength degradation index δ_s is obtained as the ratio between the maximum deviatoric stress at the current cycle, N_c, and the maximum deviatoric stress obtained from a monotonic triaxial test.

In this paper, the damage factor is expressed as follows:

$$D = \frac{N_c}{N_U} \qquad (4)$$

namely, the ratio between the current cycle, N_c, and the cycle, N_U, corresponding to the liquefaction onset, δ_f. In the beginning, $D = 0$ and $\delta_s = 1$, while at N_f, $\delta_s = \delta_f$. The strength degradation index can be seen as the multiplier of the initial strength or yield value of a "p-y" relation to account for cyclic degradation.

Therefore, this model requires the evaluation of two functions: the Wöhler curves, here represented as $\varepsilon_{zz}^{max} - N_U$ curve for strain-controlled testing, and the degradation curve expressing the relation between δ_s and the N_c, which is fully defined when the empirical curve shape parameter is given.

To investigate the impact of the particle size distribution on these parameters, a Monte Carlo Simulation of the DEM model defined in Section 3 is performed.

5.1. Sample generation

The particle size distribution (PSD) functions are generated by assuming them affected by an inherent variability as proposed by Phoon and Kulhawy (1999), hence considering the Ottawa F65 PSD as mean value and a normally distributed fluctuation as follows:

$$P_{d,i} = P_{d,i}^{F65}(1 + w_i \cdot COV_i) \qquad (5)$$

where $P_{d,i}$ is the percentage finer at the sieve diameter, d, i, $P_{d,i}^{F65}$ is the percentage finer of the experimental distribution, w_i is a random number drawn from the standard normal distribution and COV_i is the coefficient of variation.

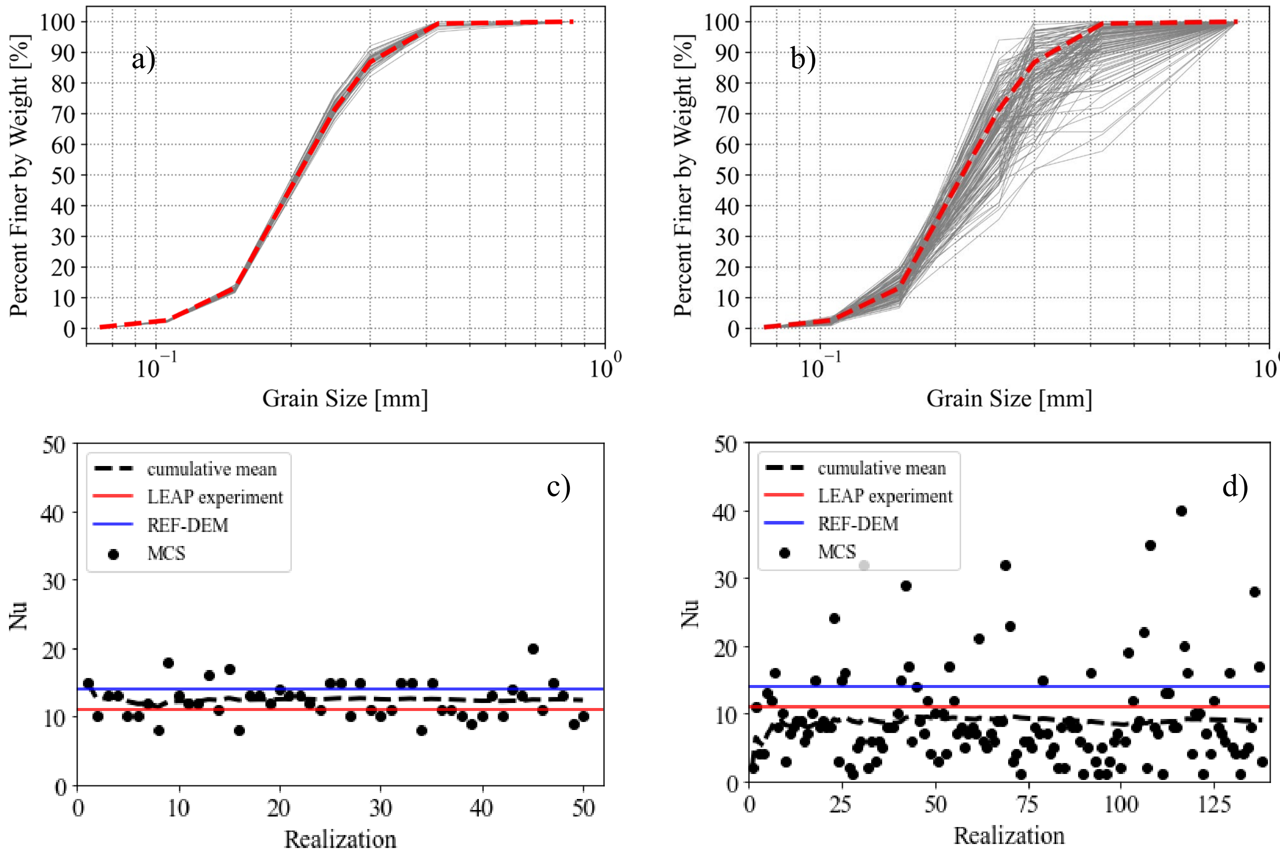

Figure 5 Monte Carlo Simulation: PSD curves for a) $COV_i = 0$ and b) $COV_i = 0.2$; Number of cycles to liquefaction ($\varepsilon_{zz}^{max} = 0.1\%$) for a) $COV_i = 0$ and b) $COV_i = 0.2$

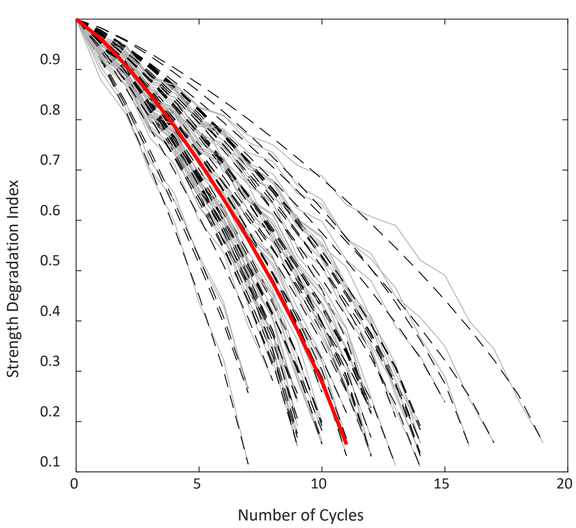

Figure 6 Strength Degradation Index curve for $COV_i = 0$ for $\varepsilon_{zz}^{max} = 0.1\%$; DEM simulation (gray continuous lines), fitting to Eq.3 (black dashed lines), mean fitting line (thick red continuous line)

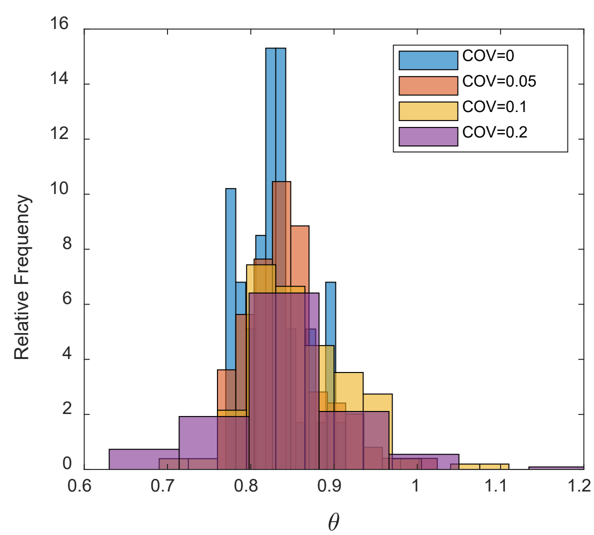

Figure 7 Distribution of the Curve Shape Parameters for several COV

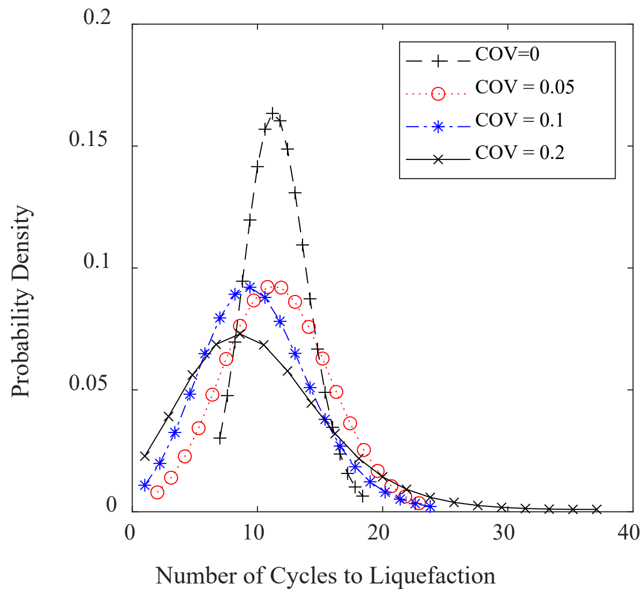

Figure 8 $\varepsilon_{zz}^{max} - N_U$ for $COV_i = 0$

Table 2 Statistics of the computed parameters for the fatigue model

COV_i	0.00	0.05	0.1	0.2
N_U^{mean}	11.31	11.30	9.27	8.53
N_U^{COV}	0.23	0.39	0.51	0.82
N_U^{min}	7	2	1	1
N_U^{max}	19	24	25	39
θ^{mean}	0.83	0.84	0.86	0.85
θ^{COV}	0.043	0.056	0.072	0.118
θ^{min}	0.77	0.77	0.7	0.7
θ^{max}	0.91	1.01	1.1	1.63

4 COV_i equal to 0, 0.05, 0.1 and 0.2 are tested to represent the inherent soil variability obtained in past studies (Phoon and Kulhawy, 1999). The generated samples for $COV_i = 0$ and $COV_i = 0.2$ are shown in Figures 5a-b, respectively; because of the random generation of particles described in Section 3.2, the mean COV_i of the generated PSD functions are calculated as at 0.029, 0.053, 0.083, and 0.145, for the 4 COVs respectively.

5.2. Calibration of the Cyclic Damage Model

Cyclic triaxial testing as described in Section 3.3 is performed for each of the generated samples. The outcome in terms of the number of cycles to liquefaction for the maximum axial strain of 0.1% is shown in Figs 5c-d for $COV_i = 0$ and $COV_i = 0.2$, respectively. It is worth noting that the cumulative mean of the number of cycles to liquefaction, N_U, has been monitored to determine the optimal number of samples for each COV. It can be observed that the dispersion of the results is higher when for the $COV_i = 0.2$ evidencing the importance of the particle size distribution on the liquefaction onset. Moreover, the cumulative mean is closer to the experimental results than the reference curve obtained through heuristic optimization. A summary of the results is presented in Table 2.

Therefore, the analyses have been elaborated to obtain the $\varepsilon_{zz}^{max} - N_U$ and δ_s - N_c curves in order to calibrate the fatigue model of Eq. (3). Figure 6 shows the variation of the strength degradation index with the increase of the number of cycles for $COV_i = 0$. The grey curves are obtained from the DEM simulations; a large dispersion of the results is obtained as reported in Table 2. The black curves are derived by using Eq. (3) in which the parameter theta has been obtained by the best-fit of each DEM curve. Apart from one outlier ($\theta = 1.63$ at COV_i=0.2), the range of θ is consistent with the experimental results on saturated sands performed by De Alba et al. 1976 ($\theta = 0.7 - 1.1$). Distribution of θ are shown in Figure 7. Therefore, when adopting Allotey and El Naggar's model, the shape parameter for Ottawa F65 sand can be assumed as random distributed variable with mean 0.845 and COV depending on the initial uncertainty on the PSD.

5.3. Analytical Probability Distribution of N_U

Because of the non-normal distribution of the computed numbers of cycles to liquefaction, N_U, an approximate analytical probability distribution function, $pZ(z)$, is obtained by using the Maximum Entropy (MaxEnt) principle (see, e.g. Batou and Soize, 2014) as follows:

$$pZ(z) = Nexp[-\lambda_0]exp\left[-\sum_{j=1}^{m} \lambda_j z^j\right] \quad (6)$$

where N is a normalizing constant, λ_j j=0..m are the coefficients of polynomial of the standardized variable z and m is the order of the truncated polynomial. Figure 8 shows the obtained CFC probability distribution functions for the 4 investigated degree of uncertainty. The MaxEnt probability density function coefficients have been determined considering the first 4 standardized statistical moments (i.e. m=4) for which satisfactory convergency has been achieved for the considered number of samples. These analytical expressions can be used to generate realizations of the $\varepsilon_{zz}^{max} - N_U$ curves for the random cyclic damage model of Eq. (3).

6. CONCLUSIONS

The Allotey and El Naggar's degradation model has been calibrated through a Monte Carlo Simulation of undrained cyclic triaxial testing performed through the Discrete Element Method. The DEM models well captured the soil degradation effect and hence, have been used to calibrate the degradation model through statistical regression analysis and the Maximum Entropy Principle to determine analytical expressions of the probability density function. Results showed that the obtained parameters are consistent with the values indicated in literature. Therefore, the DEM represents an interesting approach to extend experimental results and obtain results from a larger number of samples to be used in the calibration of continuous soil models or empirical damage models considering soil uncertainties.

7. ACKNOWLEDGEMENTS

Dr Tombari gratefully acknowledges the financial support of the Engineering and Physical Sciences Research Council (EPSRC) through the New Investigator Award EP/W001071/1 "Structural Life-Cycle Enhancement of Next-Generation Onshore and Offshore Wind Farms".

8. REFERENCES

Allotey, N., and El Naggar, M. H. (2008). "Generalized dynamic winkler model for nonlinear soil–structure interaction analysis." Canadian Geotechnical Journal, 45(4), 560–573.

Allotey, N., and El Naggar, M. H. (2007). "A consistent soil fatigue framework based on the number of equivalent cycles." Geotechnical and Geological Engineering, 26(1), 65–77.

Cundall, P. A., and Strack, O. D. (1979). "A discrete numerical model for granular assemblies." Géotechnique, 29(1), 47–65.

Maksimov, F., and Tombari, A. (2022). "Derivation of cyclic stiffness and strength degradation curves of sands through discrete element modelling." Modelling, 3(4), 400–416.

Batou, A., Soize, C. Generation of accelerograms compatible with design specifications using information theory. Bull Earthquake Eng 12, 769–794 (2014).

Phoon, K.-K., and Kulhawy, F. H. (1999). "Characterization of geotechnical variability." Canadian Geotechnical Journal, 36(4), 612–624.

Kutter. (2020). Model tests and numerical simulations of liquefaction and lateral spreading. Springer International Publishing.

ElGhoraiby, M. A., Park, H., and Manzari, M. T. (2020). "Stress-strain behavior and liquefaction strength characteristics of Ottawa F65 Sand." Soil Dynamics and Earthquake Engineering, 138, 106292.

Kozicki, J., and Donzé, F. V. (2008). "A new open-source software developed for numerical simulations using discrete modeling methods." Computer Methods in Applied Mechanics and Engineering, 197(49-50), 4429–4443.

Martin, E. L., Thornton, C., and Utili, S. (2020). "Micromechanical investigation of liquefaction of granular media by cyclic 3D DEM tests." Géotechnique, 70(10), 906–915.

Saltelli, A., Ratto, M., Andres, T., Campolongo, F., Cariboni, J., Gatelli, D., Saisana, M., and Tarantola, S. (2007). "Global Sensitivity Analysis. the Primer."

Schafhirt, S., Page, A., Eiksund, G. R., and Muskulus, M. (2016). "Influence of soil parameters on the fatigue lifetime of offshore wind turbines with monopile support structure." Energy Procedia, 94, 347–356.

Shajarati, A., Sørensen, K.W., Nielsen, S.K., Ibsen, L.B. (2012). "Behaviour of Cohesionless Soils During Cyclic Loading". DCE Technical Memorandum No. No. 14. Aalborg University.

Van Eekelen, H. A. (1977). "Single-parameter models for progressive weakening of soils by cyclic loading." Géotechnique, 27(3), 357–368.